AUT Journal of Electrical Engineering
10.22060/EEJ.2026.25442.5934

Predicting Torque Ripple and Average Torque of a Switched Reluctance Motor Using MLP and RBF Models

Siroos Hemmati[1,*], Milad Goldasteh[2], Mohsen Asadi[3], Seyed Shahrooz Hosseini[4], Sobhan Roshani[5]

[1]Associate Professor, Kermanshah University of Technology, Kermanshah, Iran.
[2]Msc, Technical National University, Kermanshah, Iran.
[3]Msc, Razi university, Kermanshah, Iran.
[4]Msc, Azad University, Kermanshah, Iran.
[5]Associate Professor, Azad University, Kermanshah, Iran.
[*]Corresponding author: s.hemmati@kut.ac.ir

Abstract:

The optimal design of a Switched Reluctance Motor (SRM) requires an accurate model. Analytical models presented for SRM do not meet required accuracy. Approximate models also have varying degrees of accuracy in predicting SRM characteristics. Hence, in this paper, two Neural Network (NN) models, Radial Basis Function (RBF) and Multilayer Perceptron (MLP), have been proposed to predict torque ripple and average torque, respectively. To train and test the models, 100 samples were extracted, 90% for training and 10% for testing. Furthermore, the Finite Element Method (FEM) has been used to solve the samples. The influencing parameters of the proposed NN models (number of hidden layers, number of neurons in hidden layers, bias, etc.) also have been determined to achieve the desired accuracy and minimal complexity. To evaluate the performance of the models, two criteria, Root Mean Square Error (RMSE) and Mean Relative Error (MRE), have been used. Both criteria indicate that the MLP model is successful in predicting torque ripple, while the RBF model excels in predicting average torque.

Keywords:

Switched Reluctance Motor, Torque, MLP, RBF, Neural Network

1. Introduction

The torque ripple and average torque are two important characteristics of SRM and are studied in the majority of SRM optimization problems [1,2]. On the other hand, several studies (for example [3] and [4]) have shown that among the various parameters related to SRM structure, the stator and rotor pole arcs are among the most influential factors affecting the torque ripple and average torque. Accordingly, the main objective of this paper is to create a relationship between the stator and rotor pole arcs and the torque ripple and average torque.

In [3], the pole arcs of the stator and rotor are optimized in order to achieve higher average torque and low torque ripple. In the mentioned study, several SRM samples with different combinations of pole arcs were investigated. The FEM model is used in the optimization process, which is time-consuming when searching for the global optimum among a large number of samples. Similarly, in [4], using only the FEM model, the inner and outer pole arcs of the stator and rotor in a double-stator SRM (DSSRM) were optimized as the main structural variables of the SRM to achieve maximum torque with low torque ripple. All models were simulated in 3-D, which makes the procedure highly time-consuming.

Due to the nonlinear behavior of SRM, approximate SRM models including artificial neural network ANN models [5,7], Fuzzy models [8,10], Statistical models [11,13] have received more attention. Among approximate models, ANNs have been widely used for modeling SRM. For example, in [14], an NN has been proposed to estimate the rotor position utilizing information related to air gap flux and phase current. The model configuration is optimized to increase its accuracy. The same approach is also used in [15] to model the magnetic field and inductance of a double layer switched reluctance motor (DLSRM). In [16], the Back-Propagation Neural Network (BPNN) was proposed for use in the SRM control system. The training samples are dynamically extracted and implemented using an online training mechanism. In this scenario, the NN is continuously updated to maintain high accuracy under various operating conditions. Simulations conducted under different conditions, such as speed variations from 500 to 1000 rpm and torque variations from 30 Nm to 50 Nm, show a small error between the actual values and the estimations. In [17], a long short-term memory (LSTM) neural

network was also used for estimating the rotor position of an SRM without sensors. The proposed network was trained using experimental data collected from a fabricated prototype at various speeds and load conditions. In that study, 600 data samples were utilized for training and testing the model. The experimental results confirm that the proposed neural network performs better in comparison to fuzzy logic and other existing models.

In [18], an improved Recurrent Neural Network (RNN) has been employed to predict the motor efficiency and average torque based on the geometry-related variable. The authors extracted 120 data samples for training and testing the proposed model. The results indicate that the proposed model has higher accuracy compared to other models. However, from the presented results, it can be observed that the RNN model does not have the same level of accuracy in predicting torque ripple and efficiency.

in the current work, two models, RBF and MLP, are tested to predict both desired characteristics (torque ripple and average torque). The results show that each model performs better in predicting one of the mentioned characteristics. More specifically, the RBF model predicts the average torque with a smaller error than the MLP, and the opposite is true for predicting the torque ripple. It should be noted that the parameters influencing the accuracy of the models (number of hidden layers, number of neurons in hidden layers, bias, etc.) also are tuned to achieve the desire accuracy with minimal complexity. Finally, it is shown that the proposed models can estimate the desired outputs with a minimum error.

The contents of this paper are as follows. In section 2 the RBF and MLP neural networks are introduced. Section 3 presents the detailed steps taken to create the models, and finally, Section 4 provides the results.

2. MLP and RBF Artificial Neural Networks

Since the MLP and RBF are extensively discussed in numerous sources, only a brief introduction is made here.

2-1- MLP

The MLP Artificial Neural Network consists of three layers: input, hidden layer(s), and output layer. The hidden layer can be composed of one or multiple layers. Increasing the number of layers affects the complexity and accuracy of the model. Furthermore, each hidden layer can have different number of neurons, that, similarly influences the model's complexity and accuracy. It should be noted that the MLP network is typically trained using the BP error method, in which the error between the predicted and actual values by is calculated using the following relation:

$$er_1 = \frac{(y_1^{actual} - y_1)^2}{2} \qquad E_T = \sum_{l=1}^{N_t} er_l \tag{1}$$

where, y_1^{actual}, y_1 and E_T are the actual output, the output predicted by the network and total error, respectively. In the BP method, the network connection weights are updated in each step. The correction process is repeated until the minimum error is reached.

2-2- RBF

The artificial neural network RBF consists of three layers: input, hidden, and output. During the training of RBF, the hidden layer in the initial network does not contain any neurons and throughout the training process, one neuron is added each time until the network reaches the target error or the number of neurons reaches its maximum. The greatest advantages of RBF are its best approximation ability and fast convergence speed. Similar to the MLP model, the number of hidden layers and the number of neurons in the hidden layers are factors affecting the model's accuracy.

3. Proposed models

This section provides details of the proposed models.

3-1- Specifications of the motor under study

As shown in Fig. 1, the motor under study is a three-phase (6/4) SRM. Motor specifications is also presented in Table 1.

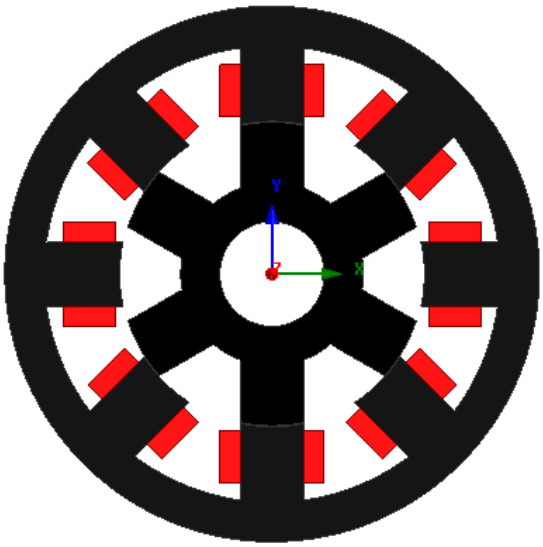

Fig. 1. Two-dimensional view of the SRM under study

Table 1. SRM specifications

Parameter	Value	Unit
Stator outer diameter	207	Mm
Stator inner diameter	116.8	Mm
Stator pole height	30.2	Mm
Rotor outer diameter	116.1	Mm
Air gap length	0.35	Mm
Number of turns	58	Turns
Stator pole arc	20	deg.
Rotor pole height	16	Mm
Rotor pole arc	24	deg.
Stack depth	171	Mm

3-2- Model configuration

Since torque ripple and average torque are two very important characteristics of the SRM, they are considered as the outputs of the model. On the other hand, considering the sensitivity analysis performed in [19], the rotor pole arc (β_r), as well as the stator pole arc (β_s) are two highly influential variables on the torque. Therefore, β_r and β_s are determined as the inputs to the model. Thus, the inputs and outputs of the proposed model are as shown in Fig. 2.

10.22060/EEJ.2026.25442.5934

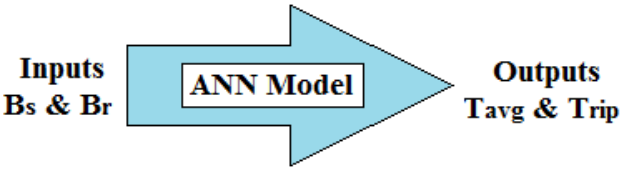

Fig. 2. Model inputs and outputs

To ensure the SRM's self-starting, the pole arc variation is limited to a specific region. The relationship between the stator and rotor pole arcs is as follows:

$$\beta_r + \beta_s \leq \frac{2\pi}{N_r} \tag{2}$$

$$\beta_r \leq \beta_s \tag{3}$$

$$\beta_s \leq \frac{2\pi}{mN_r} \tag{4}$$

where, N_r is the number of rotor poles and m is the number of phases. Hence, the range of variations of β_s and β_r are given in Table 2.

Table 2. Range of variations of variables

Variables	Range	Unit
Stator pole arc	20-25	deg.
Rotor pole arc	18-30	deg.

3-3- Data extraction

To collect the required data, the motor was simulated in the Maxwell software. A total of 100 data points were collected for model training and testing, from which 90% allocated to training and 10% to testing. It should be noted that the sampling was performed using a uniform distribution method. Before data extraction, the flux density of the motor was obtained under the worst-case scenario (10 Amperes current, rotor and stator pole arcs at their minimum values of the specified

10.22060/EEJ.2026.25442.5934

range). The resulting flux density distribution under these conditions is shown in Fig. 3(a). As can be observed, the flux density in the worst-case scenario has not exceeded the allowed value (approximately 2 Tesla). Furthermore, the magnetic flux path is shown in Fig. 3(b). It can be observed that the magnetic flux distribution in different regions of the machine is not uniform. The magnetic flux density is higher in areas such as the air gap, the corners and edges of the structure. Therefore, to increase the accuracy, the number of meshes in these regions has been increased.

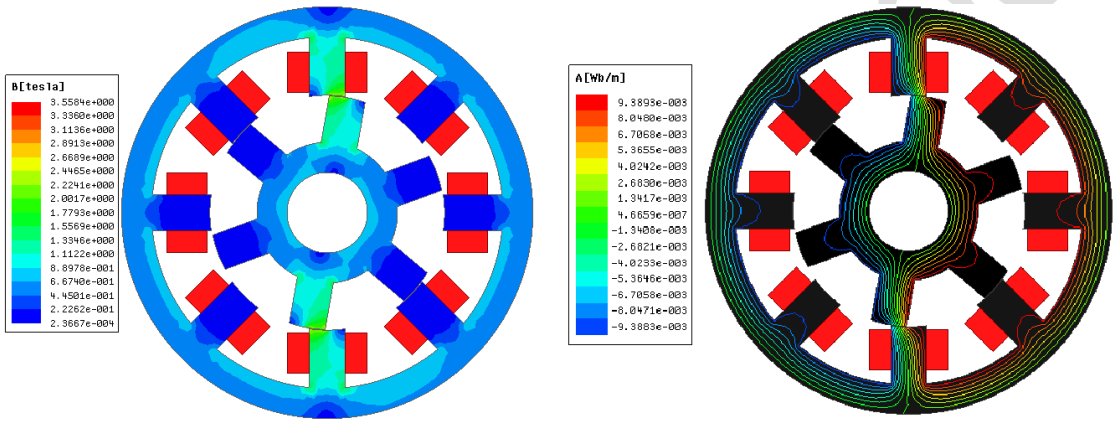

Fig. 3. flux density and magnetic flux lines: a) Distributed flux density for a current of 10 amperes, $\beta r = 18$ and $\beta s = 20$. b) The path of magnetic flux lines.

Since the proposed models predict static torque (rotor in one position), the torque curve is obtained by rotating the rotor for 30 degrees (steps of 0.5 deg) while keeping one of the phase currents at 10A. As example, three of the extracted torque curves are shown in Fig. 4. As can be seen, the value of torque ripple and average torque differ in various samples.

10.22060/EEJ.2026.25442.5934

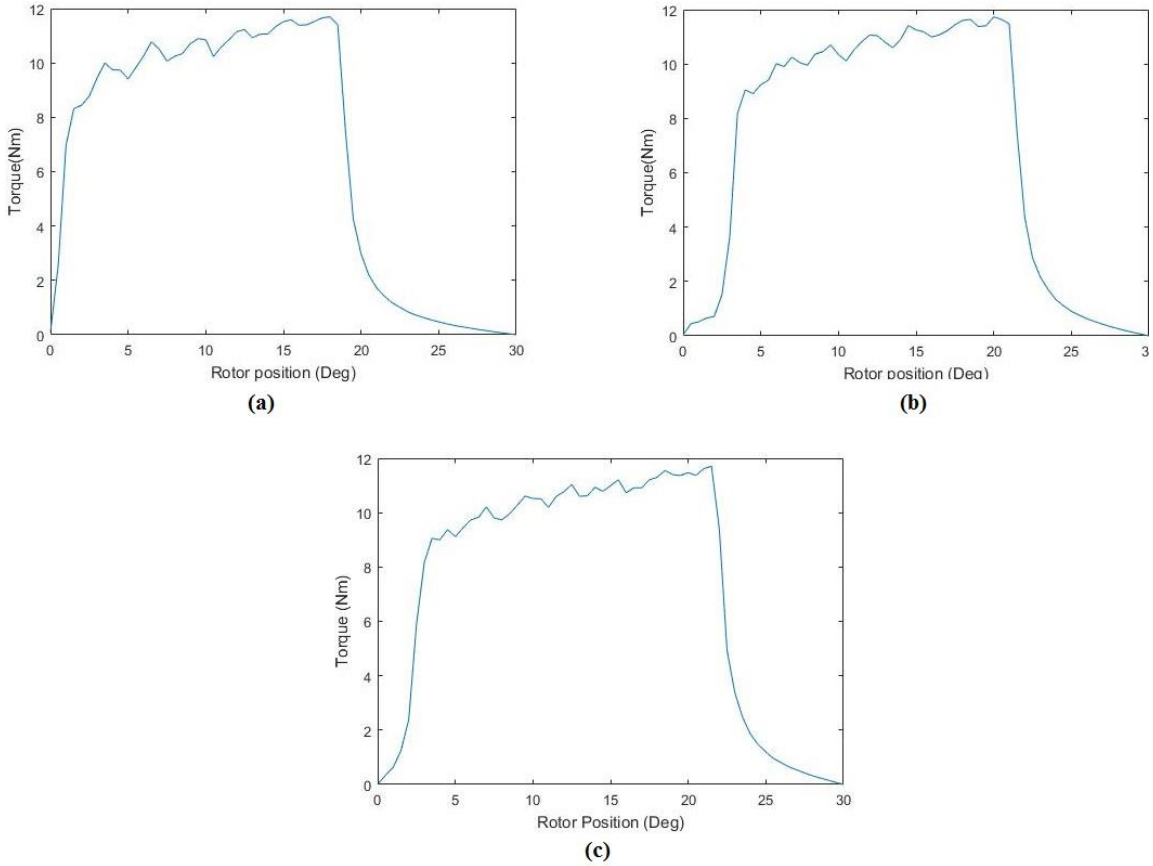

Fig. 4. Torque curves for three different SRM samples: a) $\beta r = 18$ & $\beta s = 20$. b) $\beta r = 18$ & $\beta s = 25$. C) $\beta r = 24$ & $\beta s = 20$

After obtaining the torque curve and calculating the average torque using Maxwell, the torque ripple is calculated using the following relation:

$$Ripple = \frac{T_{\max} - T_{\min}}{T_{avg}} \tag{5}$$

where, $T_{\max}$ is the maximum torque, $T_{\min}$ the minimum torque, and T_{avg} the average torque.

3-4- Specifications of the proposed models

As mentioned earlier, in the present work, the parameters influencing the accuracy of the RBF and MLP models are set to their best possible state (desired accuracy and minimum complexity). The list of these settings is presented in Table 3.

Table 3. Proposed model specifications

Parameters	MLP Model	RBF Model
Input neurons number	2	2
Output neurons number	1	1
Hidden layers number	2	2
Hidden layers neurons	8&6	8&6
Activation function	tansig	Tansig
Epoch number	1000	1000

4. Testing and final results

In this section, the error of the presented models for predicting average and ripple torque is examined. To evaluate the models, two assessment criteria, RMSE and MRE, are used. The two mentioned criteria are calculated using the following relationships.

$$RMSE = \frac{1}{N}\sum_{i=1}^{N}\sqrt{(Y_{Ri} - Y_{Pi})^2} \tag{6}$$

$$MRE = \frac{1}{N}\sum_{i=1}^{N}(Y_{Ri} - Y_{Pi}) \tag{7}$$

where, Y_{Ri}, Y_{Pi}, N are the actual output, model prediction and total number of the data, respectively. The error result for each model is reported below.

4-1- Torque ripple prediction

Here, the performance of both the RBF and MLP models in predicting the torque ripple is evaluated. The results concerning the error of the RBF and MLP models in predicting torque ripple are shown in Table 4. It can be seen that the MLP model predicts torque ripple with less error than the RBF model. Thus, the MLP model is suggested for predicting the torque ripple.

10.22060/EEJ.2026.25442.5934

Table 4. Error results of RBF and MLP models in predicting torque ripple

	MRE-Test	MRE-Train	RMSE-Test	RMSE-Train
T_{rip} – MLP	0.0046	9.8585e-05	0.6703	0.0287
T_{rip} – RBF	0.0070	0.0035	1.1374	0.66914

The performance map of the proposed model for predicting the torque ripple is also shown in Fig. 5. It is evident that the predicted data by the proposed model is very close to the actual data.

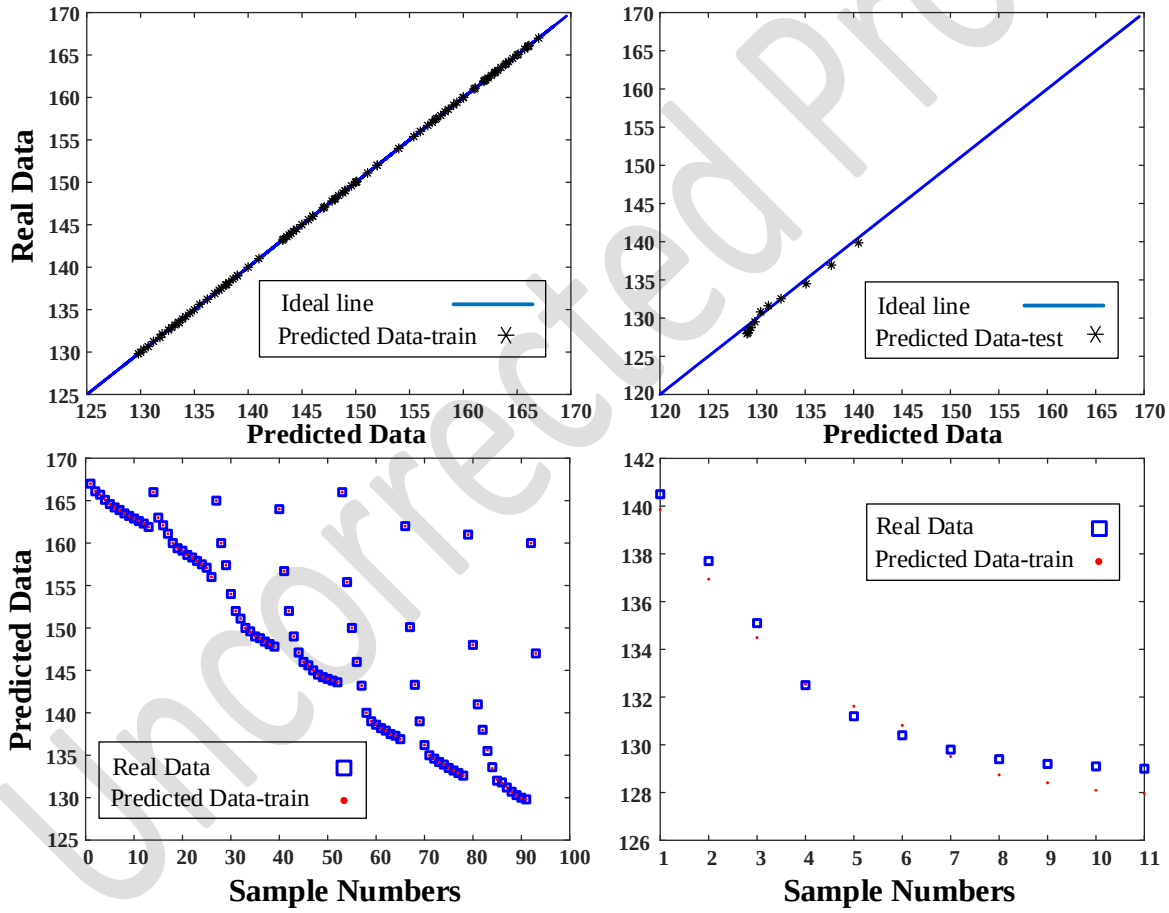

Fig. 5. The results of the proposed ANN model. Upper figures show the regression diagram of the ANN results. The lower figures show the predicted values vs. the sample numbers.

The Residual plots for torque ripple prediction are illustrated in Fig. 6. The residual plots show the difference between the real and predicted torque ripple values. The residuals are randomly

10.22060/EEJ.2026.25442.5934

distributed around zero without a clear trend, indicating that the proposed neural network model provides an unbiased prediction and captures the relationship between the input parameters and torque ripple effectively.

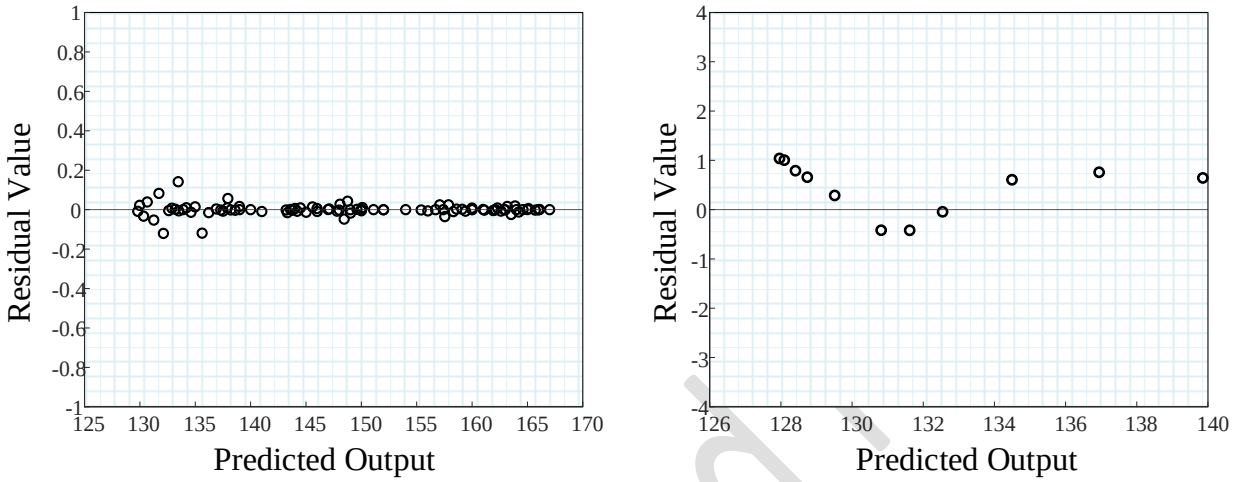

Fig. 6. Residual plots for torque ripple prediction using the proposed neural network model.

4-2- Average Torque prediction

The ability of both the RBF and MLP models in predicting the average torque is evaluated and presented in table 5. It can be seen that the RBF model predicts the average torque with less error than the MLP model. Thus, the RBF model is recommended for predicting the average torque.

Table 5. Error results of RBF and MLP models in predicting average torque

	MRE-Test	MRE-Train	RMSE-Test	RMSE-Train
T_{avg} – MLP	0.0126	5.1339e-05	0.1220	7.0183e-04
T_{avg} – RBF	0.0091	0.0062	0.0880	0.0641

The complete map showing the performance of the proposed model for predicting average torque is illustrated in Fig. 7. The diagram includes the regression of the train and test models (upper diagram). As observed from the results, the predicted data by the proposed model closely follows

10.22060/EEJ.2026.25442.5934

the actual data with high accuracy. The lower figures show the predicted values vs. the number of the samples.

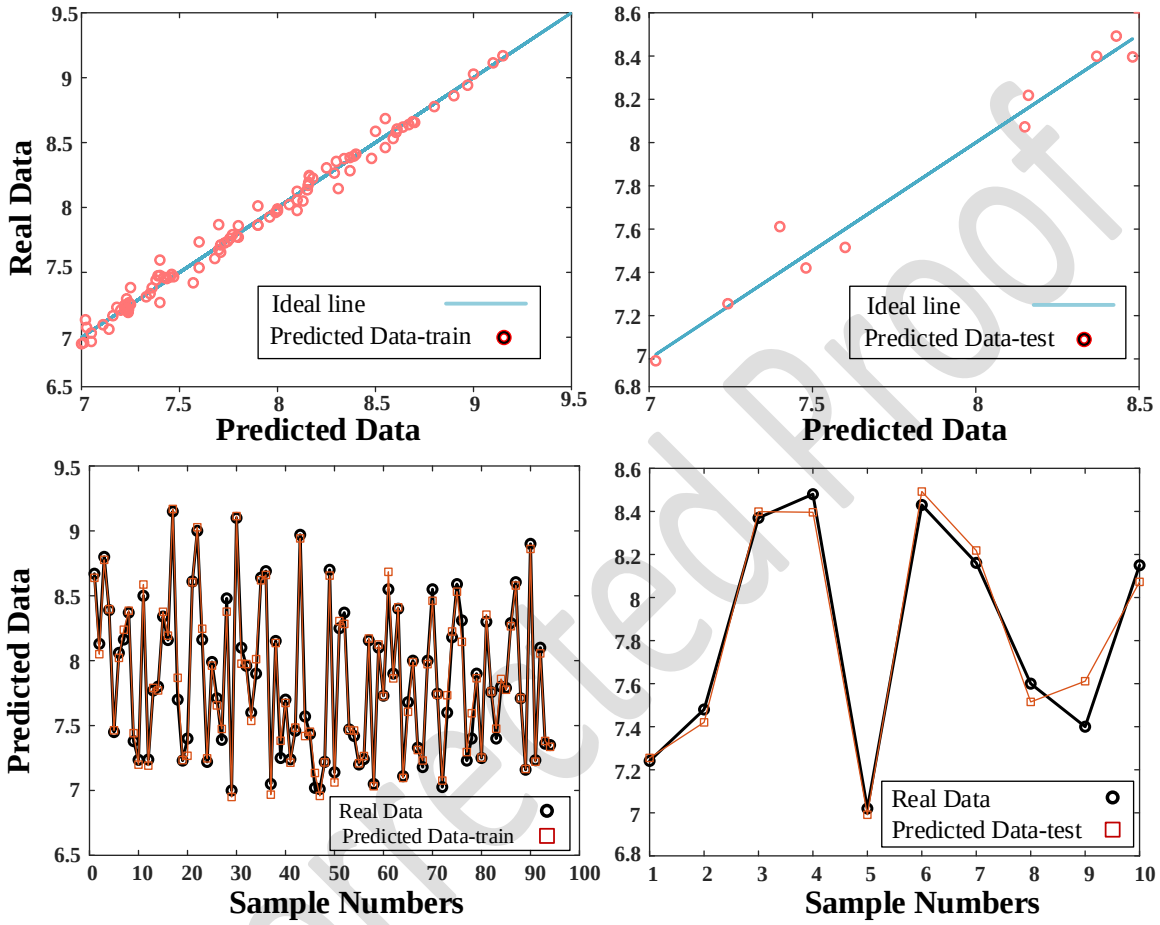

Fig. 7. The results of the proposed RBF model. Upper figures show the regression of the ANN results. The lower figures show the predicted values vs. the sample numbers.

The Residual plots for average torque prediction using the proposed RBF model are shown in Fig.8. The residual plots illustrate the difference between the real and predicted average torque values. The residuals are scattered randomly around the zero line with no clear pattern, suggesting that the proposed neural network model produces unbiased predictions and successfully represents the relationship between the input parameters and the torque ripple.

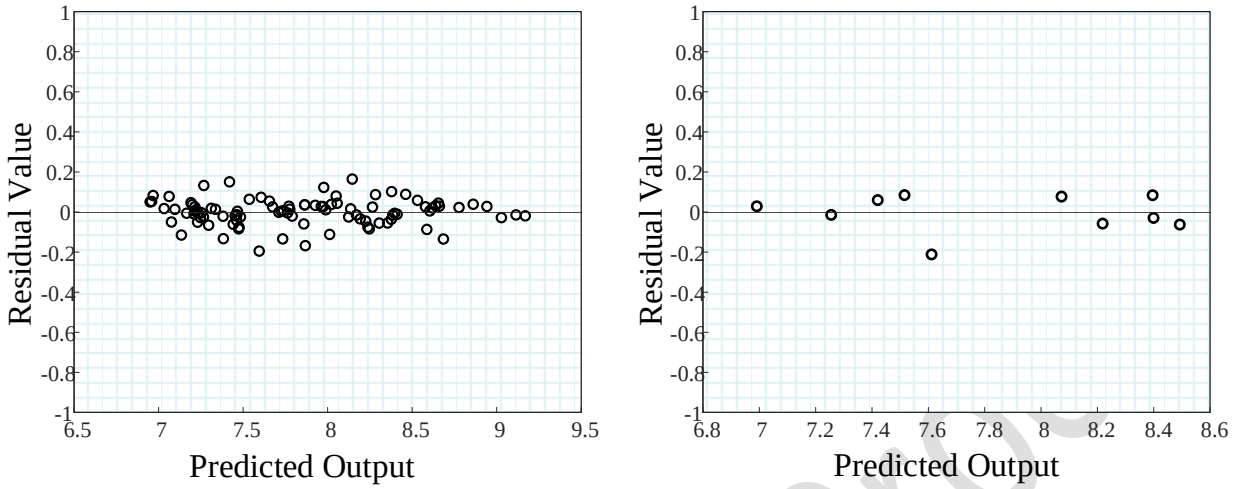

Fig. 8. Residual plots for average torque prediction using the proposed RBF model.

Conclusion

In this study, two models—RBF and MLP—were proposed for predicting torque ripple and average torque. The performance results show that the MLP model predicts the torque ripple with RMSE=0.6703 and the average torque with RMSE=0.1220. On the other hand, the RBF model predicts the torque ripple with RMSE=1.1374 and the average torque with RMSE=0.0880. Based on these results, it can be concluded that the MLP model performs better in predicting torque ripple, while the RBF model is more successful in predicting average torque.

5. References

[1] Vahedi, Payam, Babak Ganji, and Seyed Ebrahim Afjei. "Design Optimization of the Multi-layer Switched Reluctance Motor to Minimize Torque Ripple and Maximize Average Torque." AUT Journal of Electrical Engineering 56.1 (Special Issue) (2024): 95-112.

[2] Lee, Jaewook, Jeong Hun Seo, and Noboru Kikuchi. "Topology optimization of switched reluctance motors for the desired torque profile." Structural and multidisciplinary optimization 42 (2010): 783-796.

[3] N. K. Sheth and K. R. Rajagopal, "Optimum pole arcs for a switched reluctance motor for higher torque with reduced ripple," 2003 IEEE International Magnetics Conference (INTERMAG), Boston, MA, USA, 2003, pp. CP-06, doi: 10.1109/INTMAG.2003.1230356.

[4] Q. Sun, J. Wu, C. Gan, C. Shi and J. Guo, "DSSRM Design With Multiple Pole Arcs Optimization for High Torque and Low Torque Ripple Applications," in IEEE Access, vol. 6, pp. 27166-27175, 2018, doi: 10.1109/ACCESS.2018.2834901.

[5] Lu, Wenzhe, Ali Keyhani, and Abbas Fardoun. "Neural network-based modeling and parameter identification of switched reluctance motors. " IEEE transactions on energy conversion 18.2 (2003): 284-290.

[6] Wang, Libiao, et al. "Parameter Identification of Nonlinear Flux-Linkage Model for Switched Reluctance Motor Based on Chaotic Diagonal Recurrent Neural Network. " Journal of Engineering Science & Technology Review 17.2 (2024).

[7] Aydemir, Mustafa, and Halil Ibrahim Okumus. "Phase flux linkage estimation of external rotor switched reluctance motor with NARX neural network." Electrical Engineering 105.2 (2023): 1223-1233.

[8] Ouannou, Abdelmalek, et al. "Identification of switched reluctance machine using fuzzy model. " International Journal of System Assurance Engineering and Management 13.6 (2022): 2833-2846.

[9] Liu, Jian, et al. "A new modeling method for switched reluctance motor based on the fuzzy logic system. " 2018 37th Chinese Control Conference (CCC). IEEE, 2018.

[10] Ding, Wen, and Deliang Liang." Modeling of a 6/4 switched reluctance motor using adaptive neural fuzzy inference system. " IEEE Transactions on Magnetics 44.7 (2008): 1796-1804.

[11] Shin, Hye-Ung, and Kyo-Beum Lee. "Optimal design of a 1 kW switched reluctance generator for wind power systems using a genetic algorithm. " IET Electric Power Applications 10.8 (2016): 807-817.

[12] Huang, Su-Dan, et al. "Nonlinear modeling of the inverse force function for the planar switched reluctance motor using sparse least squares support vector machines." IEEE Transactions on Industrial Informatics 11.3 (2015): 591-600.

[13] Kumar, S. Suresh, and J. Jayakumar. "Torque modeling of switched reluctance motor using LSSVM-DE. "Neuro computing 211 (2016): 117-128.

[14] Yalavarthi, Amarnath, and Bhim Singh. "Sensorless Speed Control of SRM Drive Using Optimized Neural Network Model for Rotor Position Estimation." IEEE Transactions on Energy Conversion (2024).

[15] Ozden, Semih, Gokhan Manav, and Mahir Dursun. "ANN based magnetic field and inductance modeling of double sided linear switched reluctance motor." 2018 5th international conference on electrical and electronic engineering (ICEEE). IEEE, 2018.

[16] Shen, Xun, et al. "Simulation Research on no Position Control Strategy of Switched Reluctance Motor Based on On-Line Training of BP Neural Network. " 2023 International Seminar on Computer Science and Engineering Technology (SCSET). IEEE, 2023.

[17] Gecer, Bekir, Alper Nabi Akpolat, Necibe Fusun Oyman Serteller, Ozturk Tosun, and Mehmet Gol. 2026. "Data-Driven Sensorless Rotor Position Estimation for Switched Reluctance Motors Using a Deep LSTM Network" Electronics 15, no. 6: 1330. https://doi.org/10.3390/electronics15061330

[18] Zhang, Zhu, Shenghua Rao, and Xiaoping Zhang. "Performance prediction of switched reluctance motor using improved generalized regression neural networks for design optimization." CES Transactions on Electrical Machines and Systems 2.4 (2018): 371-376.

[19] Ma, Cong, and Liyan Qu. "Multiobjective optimization of switched reluctance motors based on design of experiments and particle swarm optimization. " IEEE Transactions on Energy Conversion 30.3 (2015): 1144-1153.